Direct-Write Fabrication of Wear Profiling IoT Sensor for 3D Printed Industrial Equipment

M.I.N.P. Munasinghe[a], L. Miles[b], and G. Paul[a]

[a]Centre for Autonomous Systems, University of Technology Sydney (UTS), Australia
[b]UTS Rapido, UTS, Australia
E-mail: Nuwan.Munasinghe@student.uts.edu.au, Lewis.Miles@uts.edu.au, gavin.paul-1@uts.edu.au

Abstract –

Additive Manufacturing (AM), also known as 3D printing, is an emerging technology, not only as a prototyping technology, but also to manufacture complete products. Gravity Separation Spirals (GSS) are used in the mining industry to separate slurry into different density components. Currently, spirals are manufactured using moulded polyurethane on fibreglass substructure, or injection moulding. These methods incur significant tooling cost and lead times making them difficult to customise, and they are labour-intensive and can expose workers to hazardous materials. Thus, a 3D printer is under development that can print spirals directly, enabling mass customisation. Furthermore, sensors can be embedded into spirals to measure the operational conditions for predictive maintenance, and to collect data that can improve future manufacturing processes. The localisation of abrasive wear in the GSS is an essential factor in optimising parameters such as suitable material, print thickness, and infill density and thus extend the lifetime and performance of future manufactured spirals. This paper presents the details of a wear sensor, which can be 3D printed directly into the spiral using conductive material. Experimental results show that the sensor can both measure the amount of wear and identify the location of the wear in both the horizontal and vertical axes. Additionally, it is shown that the accuracy can be adjusted according to the requirements by changing the number and spacing of wear lines.

Keywords –

IIoT; Wear Sensor; Additive Manufacturing; 3D Printing; Industry 4.0

1 Introduction

Additive manufacturing, also widely known as 3D printing [1], is the process of taking information from computer-aided designs (CAD) and transforming it into a printed physical object. Additive manufacturing has passed the rapid prototyping era and is increasingly being used to manufacture finished products.

Combining Cyber-Physical Systems (CPS) and IoT in the industrial domain has led to the fourth industrial revolution (Industry 4.0), and has enabled smart production, smart products and smart services [2]. Using Internet of Things (IoT) for industrial automation is making collaboration between automation and heterogeneous devices and systems more predictable, real-time, fault-tolerant, and closed-loop [3].

Authors of this paper are working on research and development of a 3D printer to print customisable GSS for use in the mineral industry. The focus is to develop a system to print a spiral with embedded sensors, which makes it a smart product that can have its operational conditions remotely monitored. Collected data from these smart spirals can be used to optimise production output, perform condition-based maintenance, maintain worker safety, troubleshoot issues, predict future failures and improve future products.

Measuring wear in industrial components in situ provides many advantages, e.g., the ability to make informed decisions related to: (a) adaptive control of various feeds and speeds to achieve optimum production rate; and (b) planned maintenance and identification of sudden equipment failure [4]. When considering this specific application of printed spirals, it is required that wear be monitored remotely, in situ and in real-time. Such monitoring enables a measure of the amount of wear over time and the location of such wear, and hence opens the possibility of improving future prints by refining the material or printing properties. Sensors should ideally be embedded within spirals, since downtime for inspection generally requires manual intervention and production interference, and ultimately profit loss. Since GSS are used in rural locations all around the world, including Brazil, USA, South Africa, India and Australia, using an IoT solution to gather data from various remote locations is advantageous and possible. Figure 1a shows a bank of these spirals and Figure 1b depicts the relative sizes.
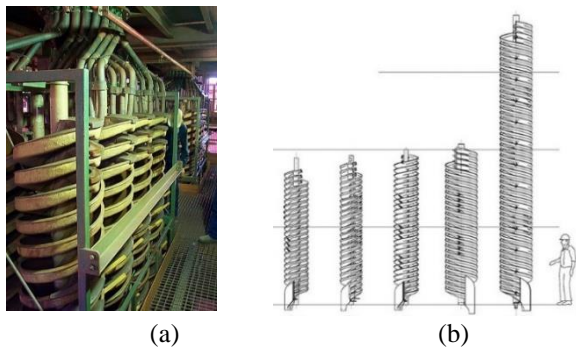
Figure 1. (a) Spiral banks in the mining site; (b) Selected spiral models and relative sizes. Source: Adapted from [5].

Direct Write (DW) refers to techniques in AM to develop various electronic and functional components using different materials without using masks or subsequent etching [6].

In this paper, a novel sensor is presented, which is developed using DW methods to measure both the amount of wear and the location of wear. The main contribution is the development of a wear sensor, which can be 3D printed directly onto industrial 3D printed components using a conductive filament to monitor the linear dimension and location of wear in situ. The rest of this paper is organised as follows: Section 2 describes related work conducted in this area; Section 3 contains the methodology of development of the sensor; Section 4 presents the results of the experiments conducted, and finally, Section 5 and Section 6 provide the discussion and conclusions respectively.

2 Related Work

Additive manufacturing has evolved beyond a rapid prototyping technology, with many industries adopting AM as their primary manufacturing process [1]. The construction industry is increasingly using AM for topology optimisation, customised parts, in situ repair, and tolerance matching [7]. Additive manufacturing is also used in medical applications such as printing customised airway stents and soft prostheses [8] [9]. Due to the unique capabilities of AM, it is possible to manufacture optimised parts which would traditionally be non-trivial to produce. The benefits of AM have been utilised by the aerospace industry to improve the power to weight ratio of autonomous aerial vehicles through the manufacture of lightweight parts. [10]. Another unique advantage of AM is the ability to combine multiple parts into a single component, reducing assembly complexity. For example, General Electric developed a 3D printed fuel nozzle for their LEAP engine, a part which traditionally was made of 20 individual parts [11].

There are many different methodologies to detect wear in industrial components [4], including, optical scanning, analysing the change in product from equipment, electrical techniques, radioactive techniques, mechanical vibrations/sound analysis, temperature measurement.

Acoustic emission (AE) is the propagation of elastic waves in the range between 0.1 and 1MHz, and these waves are generated by friction [12]. Corrosion or wear will change the AE of a component. The capture and analysis of the AE can be used to identify wear in tools [13]. Douglas et al. [12] developed an AE based wear sensor for piston rings using this method.

Fritsch et al. [14] developed a vibration based wear sensor which detects micro-mechanical resonant vibrations in the low-frequency range. The sensor was developed using a micromachined silicon structure. This sensor is used to characterise vibrations from anti-friction bearings of calendar rolls mainly used in the textile industry.

Researchers have used various electrical based methods to measure wear in industrial components. Bödecker et al. [15] developed a resistance based sensor which can detect wear in the cylinders of diesel engines. Without this kind of in situ sensor, the engine must be decommissioned to inspect the engine for wear, which incurs significant resource costs. This sensor is manufactured with a conductive layer between the two insulating layers, and this conductive layer is constructed in the form of resistive loops. A change of the resistance as these loops are worn away provides a measure of wear. Ruff and Kreider [16] developed a wear sensor using vacuum deposited thin-films. The sensor package consists of two conductive layers that lie on top of the thermocouple layer separated by insulating layers. This sensor can also be used as a temperature sensor. Another thin film-based wear sensor for cutting tools developed by Holger et al. [17] uses a coating technique for the real-time measurement of wear. This sensor is also based on parallel connected electrical resistors. The wear indicator developed by Dyck et al. [18] can be used to measure a wear surface as well as the coefficient of friction for different types of coated geometries. This indicator slides a specimen material through electrical contacts to detect wear.

The proposed method for the wear sensor in this paper includes directly creating conductive traces on the material using a carbon-based composite material. There are many DW methods, with the most common ones being inkjet, aerosol jet, and photolithography methods. Le et al. [19] used inkjet-printed graphene to develop a gas sensor which can detect NH_3 and CO gasses. This sensor is a low-cost, self-powered, battery-less, wireless sensor based on radio-frequency identification (RFID) technology. Micro-scale aerosol-

jet graphene-based additive manufacturing process, which is developed by Jabari et al. [20], uses graphene ink with a particle size below 200nm, to deposit thin graphene layers. Moreover, their results show that this process is capable of printing interconnects with widths in the range of 10-90 μm and with resistivity as low as 0.018 Ω cm. Shen et al. [21] developed a temperature sensor based on extrusion DW techniques, which used a micron-level platinum layer on top of an alumina substrate to print the sensor.

In the area of DW wear sensors, Shen et al. [22] developed a high-resolution wear sensor based on parallel silver interconnects. This process requires heat treatment of the printed part to achieve full performance. In this method parallel conductive lines contain parallel resistors, and when wear occurs, conductive interconnects are progressively removed, and the resistance changes. By measuring the resistance, it is possible to identify the level of wear. Dardona et al. [6] used the same method and tested it with both printed resistors and commercial resistors (Figure 2).

One significant drawback of these methods is an inability to determine the location of wear accurately. Also, they require additional steps and technology to embed traditional resistors and to perform post-treatment of the printed parts. Therefore, the authors propose a new wear sensor design with carbon-based material, which can measure the wear as well as the location of the wear, and does not require the embedment of traditional resistors nor post-treatment.
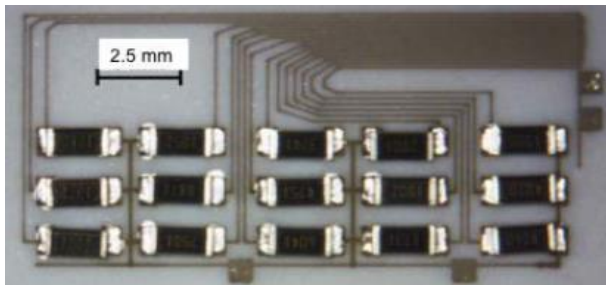

Figure 2. Printed wear sensor with commercial resistors. Source: Adapted from [6].

3 Methodology

The overall project goal is to create a large-scale printer which can 3D print a GSS. Currently, a one-third scale prototype (build volume of 220 x 1200mm) is being tested to verify the printing method. Future stages of the project will focus on constructing the full-scale eleven degrees of freedom multi-material FDM 3D printer (build volume of 700 x 2000mm). This section provides details about the materials and methodology used to develop and embed the wear profiling sensor into the printed GSS.

3.1 Design Principles

3.1.1 Conductive Filament

In order to print the conductive traces, a carbon powder blended with polylactide (PLA) is used. The volume resistivity of the moulded resin without printing is 15 Ω cm. 3D printed parts which are perpendicular to the layers along the X-Y axis have 30 Ω cm resistivity and along with the Z-axis 115 Ω cm. The nozzle temperature of the printer is 195C – 225C and heated bed temperature is in the range of 25C – 60C.

Different allotropes of carbon attracted significant interest in various types of applications in AM. The main reason is it is suitable for low-cost, large-volume applications [23]. For the developed printer project to be successful, it must be possible to produce a GSS in an equal or more economical way than traditional methods, therefore, using silver-based materials in wear sensors like Shen et al. [22] or Dardona et al. [6] is undesirable due to cost considerations. On the other hand, using carbon-based polymer composites has advantages over metal based or metal alloys. Some advantages include the lack of additional processing steps like thermal annealing, ease of printing, readily accessible technology, and longer shelf-life (years) [24].

3.1.2 Design of Printed Traces

The conductive traces shown in Figure 3 are printed using the conductive material mentioned in the previous section. The dimensions of the traces are 20x40x2mm. The number of traces can be determined based on the required wear measurement resolution. Figure 4 shows how multiple conductive layers are printed vertically aligned with each other and the intermediate insulating layers is PLA material. The number of layers can be changed according to the required wear resolution. R_X $(X = 1, ... ,4)$ represent the resistance of each trace and $R_{LX}(X = 1, ... ,4)$ represent total individual resistance of each layer. L_X $(X = 1, ... ,4)$ represents the length of each trace as marked. $W_X(X = 1, ... ,4)$ represent different locations wear can occur.
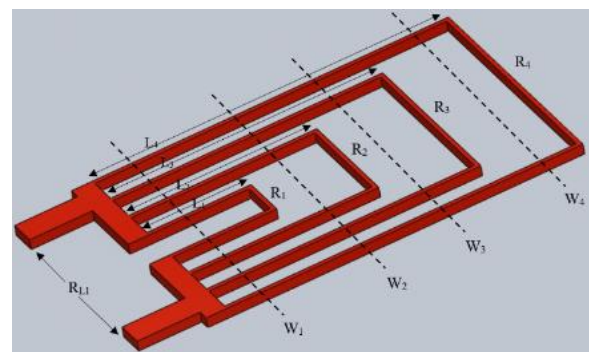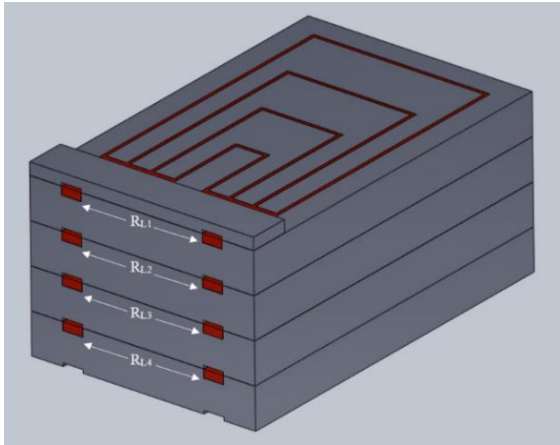

Figure 3. Printed traces in one layer.

Figure 4. Printed traces in four layers.

3.1.3 Measurement and Localisation of Wear

Since all the traces in one layer are parallel with the terminals, the total resistance of the first layer can be calculated using the Equation (1). Likewise, Equation (1) applies to each trace component in each layer.

$$\frac{1}{R_{L1}} = \frac{1}{R_1} + \frac{1}{R_2} + \frac{1}{R_3} + \frac{1}{R_4} \tag{1}$$

Without any wear, the resistance of the traces in all four layers will be equal. It is then assumed that wear occurs along W_2 line in layer one and is only just thick enough to cut through the first layer without reaching traces in layer 2. In this case, R_{L1} will be equal to R_1. Since the resistance of each traces are known, it is possible to predict that the wear occurs at a distance at least greater than L_1 but less than L_2. If wear occurs along with W_3 line, R_{L1} will be equal to the total parallel resistance of R_1 and R_2. Then by measuring the resistance, it is possible to predict that wear occur at a distance greater than L_2 but less than L_3. Likewise, by measuring the resistance, it is possible to predict the wear location within one layer. Table 1 provides a summary of the detection of the wear locations based upon the resistance in one layer.

Table 1. Wear location and resistance in one layer.

Wear Line (W_X)	Total Resistance (R_{L1})	Wear Location (x)
W_1	∞	$x < L_1$
W_2	R_1	$L_1 < x < L_2$
W_3	$\dfrac{R_1 R_2}{R_1 + R_2}$	$L_2 < x < L_3$
W_4	$\dfrac{R_1 R_2 R_3}{R_2 R_3 + R_1 R_3 + R_1 R_2}$	$L_3 < x < L_4$

The depth of the wear can be identified since the trace resistance in each layer is measured independently. Table 1 shows that in each layer, the wear distance can be estimated, which provides details of the wear profile.
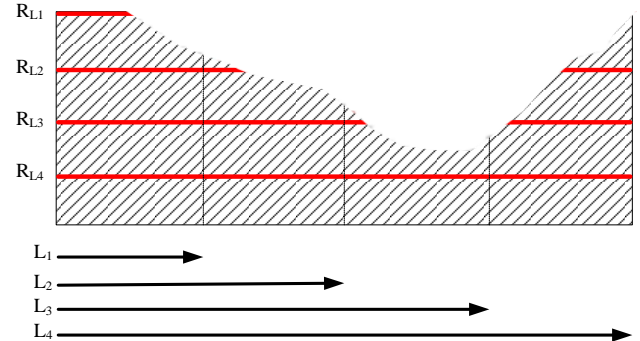

Figure 5. Cross section of the sensor with wear.

Figure 5 shows a vertical cross-section of the sensor with example wear. Table 2 summarises the possible resistance values for this wear profile and the predicted wear location.

Table 2. Wear location according to the measured resistance in each layer.

Resistance (R_{LX})	Wear Location (x)
∞	$x < L_1$
R_1	$L_1 < x < L_2$
$\dfrac{R_1 R_2}{R_1 + R_2}$	$L_2 < x < L_3$
$\dfrac{R_1 R_2 R_3 R_4}{R_2 R_3 R_4 + R_1 R_3 R_4 + R_1 R_2 R_4}$	No Wear

3.2 Sensor Accuracy

The accuracy of the estimation of the wear location depends on the number of wear lines and the maximum length of the traces in each layer. Equation (2) quantifies this error and n_x is the number of lines and L is the length of the traces.

$$\Delta x = \frac{L}{n_x} \tag{2}$$

The accuracy of the amount of wear depends on the number of wear trace layers printed and the thickness of the material. Actual production sensors will not have traces on the top surface but one below the top. Equation (3) quantifies this error.

$$\Delta y = \frac{H}{n_y + 1} \tag{3}$$

where H is the thickness of the print, and n_y is the number of layers.

4 Experiment Results

4.1 Printing Process

Three printing methods were considered to produce the printed sensor: printing on a multi-material printer; printing components separately and assembling; pausing prints; and embedding printed components into print. To reduce material wastage and print time the sensor was printed separately and assembled, irrespective of the method the functionality of the sensor is the same. The main reason for selecting the assembly method was to prevent the use of a material purge tower and to remove the need to pause the print to embed components. Figure 6 shows the assembled wear sensor.

Each component was printed using the Creality CR-10, with the following print settings, layer thickness 0.1mm, layer width 0.4mm, print speed 60mm/s. The trace components were printed using Protopasta conductive filament, with a print temperature of 220 °C, bed temperature of 60 °C, 100% infill. The insulating layer was printed using PLA filament and a nozzle temperature of 185 °C, bed temperature of 60 °C, 20% infill.
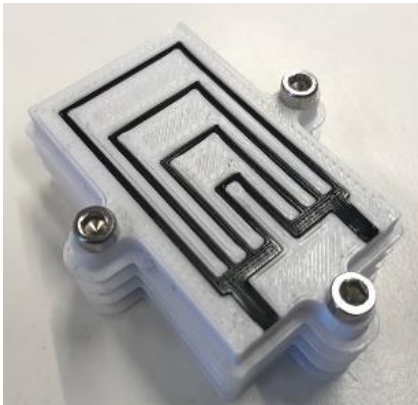

Figure 6. Printed wear sensor.

4.2 Resistance Comparison Between Multiple Prints

To determine the resistance variance across multiple conductive prints, 25 conductive traces printed as in Figure 7 and specific resistance of these traces were measured, and the standard deviation was 0.1005 kΩ. Results are shown in the graph in Figure 8, and according to the results, the resistance between multiple prints are relatively consistent.
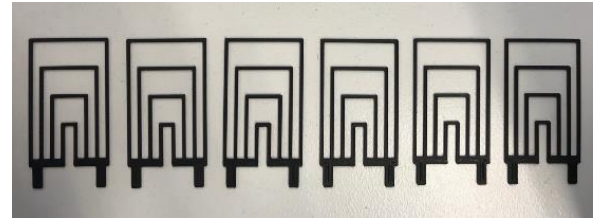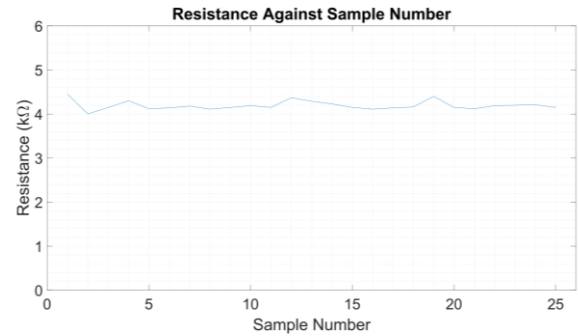

Figure 7. Multiple printed conductive traces.

Figure 8. Total resistance against sample number.

4.3 Relationship Between Resistance and Location

The resistance values need to be determined as shown in Table 1 column 2 to identify the wear location. Printed traces were disconnected to simulate wear, as shown in Figure 9, and the resistance was measured. Results are summarised in Table 3 and the trend is shown in Figure 10.
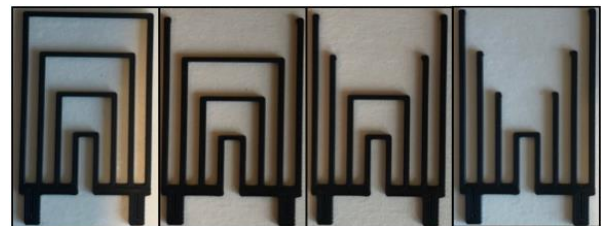

Figure 9. Resistance measurement related to different wear lines.

Table 3. Wear location and resistance in one layer

Wear Line (W_X)	Total Resistance $(R_{L1}\ k\Omega)$	Wear Location $(x\ mm)$
No Wear	4.17	None
W_4	4.83	$25 < x < 33$
W_3	5.41	$17 < x < 25$
W_2	7.23	$9 < x < 17$
W_1	∞	$x < 9$

Table 4. Predicted and actual wear locations according to the measured resistance in tested wear profiles.

Test No.	Resistance After Wear ($k\Omega$)				Actual Wear Line			Predicted Wear Line		
	R_{L1}	R_{L2}	R_{L3}	R_{L4}	Layer 1	Layer 2	Layer 3	Layer 1	Layer 2	Layer 3
1	5.45	4.82	4.29	4.10	W_3	W_4	−	W_3	W_4	−
2	5.49	5.48	5.43	4.13	W_3	W_3	W_3	W_3	W_3	W_3
3	∞	∞	4.14	4.10	W_1	W_1	−	W_1	W_1	−
4	∞	∞	7.66	4.13	W_1	W_1	W_2	W_1	W_1	W_2
5	7.20	4.18	4.11	4.16	W_2	−	−	W_2	−	−
6	7.28	7.25	4.20	4.14	W_2	W_2	−	W_2	W_2	−

Figure 10. Resistance relative to broken wear lines.

Figure 11. Wear profiles: (a) Test 1; (b) Test 2; (c) Test 3; (d) Test 4; (e) Test 5; (f) Test 6.

4.4 Results with Different Wear Profiles

Table 4 summarises the test results with different wear profiles and actual and predicted wear locations. Dashes in the table represent "no wear". There was no wear for layer 4 in actual wear and predicted wear and therefore excluded from the table. Figure 11 shows different wear profiles tested. Wear location is predicted by comparing the resistance values of each layer to the values in Table 3 and selecting the closest location. In Figure 11, dash lines show the lengths of each traces (L_X) measured from left to right and W_x represents the wear line locations as in Figure 3.

According to the results above, it is evident that the proposed method provides accurate results for different wear profiles. Resistance values were measured in 25 printed traces to identify the resistance changes between multiple prints and the standard deviation was 0.1005 $k\Omega$. Therefore, using this method as wear detection has good accuracy between multiple sensors as well.
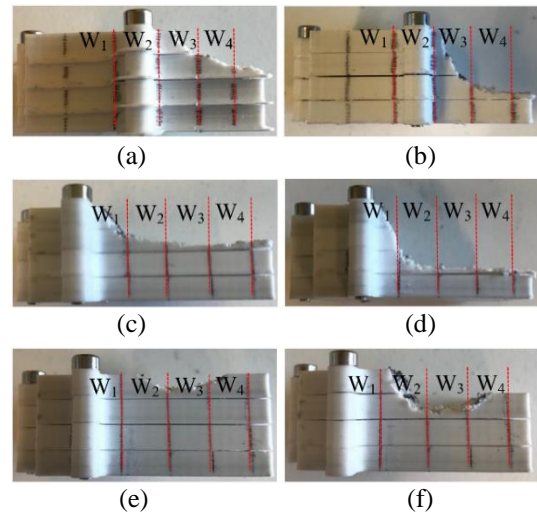
5 Discussion

The current design enables the measurement of the linear distance to wear values relative to one axis, parallel to W_1. These measurements can determine the wear profile relative to the datum axis, however, the tested configuration cannot determine wear profiles of the opposing side. It will be interesting to investigate the use of stacked sensors with opposing trace directions as shown in Figure 12. Such a sensor would introduce two datum axes rather than one, enabling the wear profile to be measured from either side. An additional benefit is that this configuration would allow the complete 2D cross-sectional profile of the wear area to be measured. The configuration could be extended by stacking sensors adjacent to each other, enabling a 3D map of the wear profile to be generated.
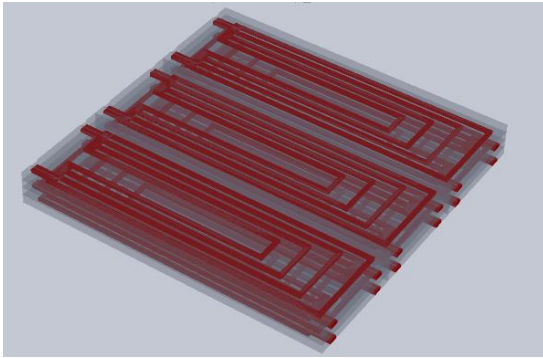
Figure 12. Suggested multi-assembly to get 3-dimensional wear profile.

6 Conclusion

The development of smart spirals, which can self-monitor operational conditions and collect data to improve future manufacturing processes, is underway. A measurement of spiral wear can help to predict its lifetime, and localising the wear provides valuable information about how to improve production. This paper has presented a novel embedded 3D printed wear sensor that can be used to measure both the location and severity of wear. The sensor is composed of printed traces using carbon-based filament, and experimental results have confirmed that real-time resistance measurements in each layer enable the location and severity of the wear to be determined accurately. By designing and printing an enhanced printed pattern it is possible to get a three-dimensional view of the wear. Future work will investigate alternative sensor configurations that will enable the wear profile to be determined in any orientation, and the integration of robustness against various wear conditions.

7 Acknowledgment

References

[1] K. V Wong and A. Hernandez, "A Review of Additive Manufacturing," *ISRN Mech. Eng.*, vol. 2012, no. Article ID 208760, p. 10, 2012.

[2] M. Wollschlaeger, T. Sauter, and J. Jasperneite, "The Future of Industrial Communication: Automation Networks in the Era of the Internet of Things and Industry 4.0," *IEEE Ind. Electron. Mag.*, vol. 11, no. 1, pp. 17–27, 2017.

[3] H. P. Breivold and K. Sandström, "Internet of Things for Industrial Automation -- Challenges and Technical Solutions," in *2015 IEEE International Conference on Data Science and Data Intensive Systems*, 2015, pp. 532–539.

[4] N. H. Cook, "Tool wear sensors," *Wear*, vol. 62, no. 62, pp. 49–57, 1980.

[5] M. Technologies, "Gravity Separation," 2015. [Online]. Available: https://mineraltechnologies.com/process-solutions/equipment-design-selection/gravity-separation. [Accessed: 16-Jan-2019].

[6] S. Dardona, A. Shen, and C. Tokgoz, "Direct Write Fabrication of a Wear Sensor," *IEEE Sens. J.*, vol. 18, no. 8, pp. 3461–3466, 2018.

[7] D. D. Camacho *et al.*, "Applications of Additive Manufacturing in the Construction Industry – A Prospective Review," in *ISARC. Proceedings of the International Symposium on Automation and Robotics in Construction*, 2017, vol. 34, pp. 1–8.

[8] G. Z. Cheng *et al.*, "3D Printing and Personalized Airway Stents," *Pulm. Ther.*, vol. 3, no. 1, pp. 59–66, 2017.

[9] Y. He, G. Xue, and J. Fu, "Fabrication of low cost soft tissue prostheses with the desktop 3D printer," *Sci. Reports (Nature Publ. Group)*, vol. 4, p. 6973, Nov. 2014.

[10] E. P. Flynn, "Low-cost approaches to UAV design using advanced manufacturing techniques," in *2013 IEEE Integrated STEM Education Conference (ISEC)*, 2013, pp. 1–4.

[11] Y. Tadjdeh, "3D Printing Promises to Revolutionize Defense, Aerospace Industries," *Natl. Def.*, vol. 98, no. 724, pp. 20–23, Mar. 2014.

[12] R. M. Douglas, J. A. Steel, and R. L. Reuben, "A study of the tribological behaviour of piston ring/cylinder liner interaction in diesel engines using acoustic emission," *Tribol. Int.*, vol. 39, no. 12, pp. 1634–1642, 2006.

[13] L. Henrique, A. Maia, A. Mendes, W. Luiz, W. Falco, and A. Rocha, "A new approach for detection of wear mechanisms and determination of tool life in turning using acoustic emission," *Tribol. Int.*, vol. 92, no. 92, pp. 519–532, 2015.

[14] H. Fritsch *et al.*, "A low-frequency micromechanical resonant vibration sensor for wear monitoring," *Sensors and Actuators*, vol. 62, pp. 616–620, 1997.

[15] A. Bödecker, C. Habben, A. Sackmann, K. Burdorf, E. Giese, and W. Lang, "Manufacturing of a wear detecting sensor made of 17-4PH steel using standard wafer processing technology," *Sensors Actuators, A Phys.*, vol. 171, no. 1, pp. 34–37, 2011.

[16] A. W. Ruff and K. G. Kreider, "Deposited thin-film wear sensors: Materials and design," *Wear*, vol. 203, pp. 187–195, 1997.

[17] H. Lüthje, R. Bandorf, S. Biehl, and B. Stint, "Thin film sensor for wear detection of cutting tools," *Sensors and Actuators*, vol. 116, no. September 2003, pp. 133–136, 2004.

[18] T. Dyck, P. Ober-Wörder, and A. Bund, "Calculation of the wear surface and the coefficient of friction for various coated contact geometries," *Wear*, vol. 368–369, pp. 390–399, 2016.

[19] T. Le, V. Lakafosis, Z. Lin, C. P. Wong, and M. M. Tentzeris, "Inkjet-Printed Graphene-Based Wireless Gas Sensor Modules," in *Electronic Components and Technology Conference (ECTC)*, 2012, pp. 1003–1008.

[20] E. Jabari and E. Toyserkani, "Micro-scale Aerosol-jet Printing of Graphene Interconnects - ResearchGate.pdf," *Carbon N. Y.*, vol. 91, pp. 321–329, 2015.

[21] A. Shen, S. B. Kim, C. Bailey, A. W. K. Ma, and S. Dardona, "Direct Write Fabrication of Platinum-Based Thick-Film Resistive Temperature Detectors," *IEEE Sens. J.*, vol. 18, no. 22, pp. 9105–9111, 2018.

[22] A. Shen, D. Caldwell, A. W. K. Ma, and S. Dardona, "Direct write fabrication of high-density parallel silver interconnects," *Addit. Manuf.*, vol. 22, pp. 343–350, Aug. 2018.

[23] W. J. Hyun, E. B. Secor, M. C. Hersam, C. D. Frisbie, and L. F. Francis, "High-resolution patterning of graphene by screen printing with a silicon stencil for highly flexible printed electronics," *Adv. Mater.*, vol. 27, no. 1, pp. 109–115, 2015.

[24] S. W. Kwok *et al.*, "Electrically conductive filament for 3D-printed circuits and sensors," *Appl. Mater. Today*, vol. 9, pp. 167–175, 2017.